TIDBIT – Thruster In-Space Diagnostics with Bus Integrated Telemetry

IEPC-2019-A-784

Presented at the 36th International Electric Propulsion Conference
University of Vienna • Vienna, Austria
September 15-20, 2019

Taylor S. Matlock[1], William R. Crain, Jr.[2], Thomas J Curtiss[3], Dan J. Mabry[4], Vincent J. Bilardo[5] and Rostislav Spektor[6]
The Aerospace Corporation (TAC), El Segundo, CA, USA, 90245

Abstract: Beginning with a prescient alert sounded by our late friend and colleague, Dave Byers, in 2009, Facility Effects exhibited by Electric Propulsion (EP) Systems have been a major concern in the EP community. Generally, Facility Effects are differences in thruster performance and behavior in the ground test environment and space environment. A major impediment to characterizing Facility Effects for different propulsion systems is a paucity of flight data taken in the space environment that can be compared with ground test data. Very few missions include the standard EP plasma diagnostics used to characterize EP thrusters. Consequently, flight data has largely been limited to relatively indirect data from Power Processing Unit telemetry. The Aerospace Corporation (TAC) has initiated a program to develop a plasma diagnostic tool (TIDBIT) intended to facilitate the generation of more flight data on EP Propulsion Systems, particularly on first flight missions. TIDBIT is an inexpensive, modular system of four probes either remotely located near the thruster or integrated into the face of a power/communication unit designed in a 1U cubesat form factor. Critical design elements and diagnostics capabilities will be summarized as well as preliminary thruster plume ground test data from a Retarding Potential Analyzer/Langmuir Probe element on a 1kW Hall thruster. We will discuss a variety of probes that can be developed that are compatible with the power/communication unit. Aerospace intends to make TIDBIT widely available to the EP community.

I.Introduction

GROUND tests never fully capture the on-orbit behavior of Electric Propulsion (EP) systems for a variety of reasons. These Facility Effects include changes in the shape and location of ion acceleration in Hall thrusters due to finite pumping of the propellant and backsputter contamination of ion engine grids. Despite careful scrutiny over the past decade and more[1-7], the mechanisms and mitigations for Facility Effects are not fully understood. It is possible to exhaustively characterize the effects of increasingly finite facility size and pumping on the ground, but difficult to characterize operation toward the infinite size and pumping of space without making such measurements on-orbit.

1 Senior Member of the Technical Staff, Propulsion Science Department, TAC, taylor.s.matlock@aero.org
2 Principal Engineer/Scientist, Electrical and Software Engineering Department, xLab, TAC, william.r.crain@aero.org
3 Director, Propulsion Science Department, Propulsion Technical Engineering Staff, Electric Propulsion & Plasma Science, TAC, tom.j.curtiss@aero.org
4 Director, Electrical and Software Engineering Department, xLab, TAC, dan.j.mabry@aero.org
5 Senior Project Leader, Human Exploration & Space Flight, TAC, vincent.j.bilardo@aero.org
6 Electric Propulsion and Plasma Sciences Laboratory Manager, Propulsion Science Department, TAC, rostislav.spektor@aero.org

Some two hundred spacecraft have flown EP systems to date, yet we are aware of fewer than ten flights with plasma diagnostics – only three flights are known with publicly available data[14-16], and several others with restricted access (as reviewed by Johnson *et al*[17]). Ground tests demonstrate that the variety of design features found on Hall thrusters alter each system's response to Facility Effects[1-4], i.e. each thruster variant exhibits different Facility Effects, recommending at least some degree of on-orbit plasma characterization for every Hall thruster system.

We cannot close the gap between ground tests and flight without flight data from the same plasma diagnostics used on ground. Ideally a single flight diagnostic package design would be used in qualification testing and in flight for all Hall thruster variants without prior flight data, with at least one measurement made in a predefined region proximal to the thruster on all flights. Adoption of such a standard would generate consistent ground and on-orbit data, allowing for the direct comparisons necessary to validate ground test methods.

An industry standard diagnostic package would need to be compact, light, low-power and economical to promote adoption and it would need to be flexible, to work on a variety of bus platforms. It would also need to be capable to be perceptive to the subtler changes in operational characteristics. Here we will present the conceptual design of a flight diagnostic package - named the Thruster In-Space Diagnostics with Bus Integrated Telemetry (TIDBIT) – intended to address these needs. This design is the initial product of a program initiated at The Aerospace Corporation aimed at providing a small, modular, economic diagnostic package that can be broadly distributed to the aerospace community to advance our understanding of Facility Effects.

The following begins with a discussion of the conceptual design of the TIDBIT system, its electronics boards and sensor options. A prototype sensor design is presented which can act as both a retarding potential analyzer and Langmuir probe. Initial ground test results for the prototype sensor are presented and discussed.

II. Conceptual Design

The goal of the TIDBIT conceptual design is to create an inexpensive, capable and versatile flight diagnostic framework for EP devices. Weight, size and power consumption should all be minimized while maintaining the main capabilities sought for in a recent NASA RFI for a Solar Electric Propulsion (SEP) Plasma Diagnostic Package (PDP). The entire package fits inside a 1U form factor which opens the door to flight demonstration as a secondary payload.

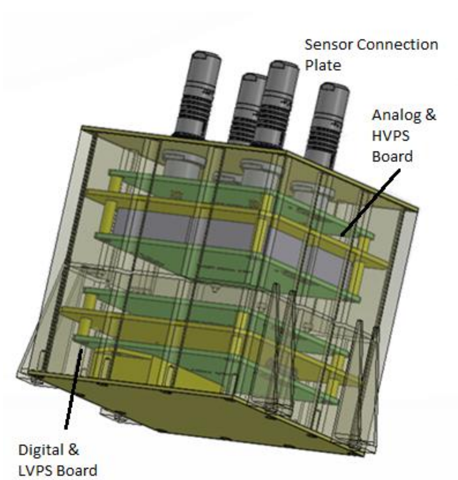

Figure 1. TIDBIT concept in 1U

A. System Architecture

TIDBIT consists of three segregated subsystems: the sensor package, the analog processing board and the digital processing board. A variety of sensor types are of interest to EP system monitoring and the precise tools needed for a mission may not be captured in a one-size-fits-all solution. However, Langmuir probes (LP's) and Retarding Potential Analyzers (RPA's) are ubiquitous in both ground and (the few) flight tests, are simple and compact, and require similar electronics – making these two sensors our leading candidates for a mission-agnostic diagnostic package. These two probe types received the highest score for value and need in a recent industry study[17.]

The conceptual design presented here is centered on the premise of control and data acquisition for Langmuir probes and RPA's from a common electronics box. The baseline design has slots for 4 sensors which can be selectable between LP's, RPA's or LP/RPA hybrids without any change to the electronics boards.

The basic architecture is shown in notional 1U form in Fig. 1 and schematically in Fig. 2. The analog processing board (APB) which contains the high voltage power supplies (HVPS) is in a separate enclosure from the digital processing board (DPB) with low voltage power supplies (LVPS) to prevent electromagnetic interference. The APB enclosure is bounded on one side by the sensor connection plate which is shown in Fig. 1 with a representative connector for cables that allow sensors to be distributed to their spacecraft-dependent locations. A demonstration unit would likely have the sensors integrated directly to the sensor connection plate.

The schematic of Fig. 2 illustrates the control/telemetry flow for a scenario using 2 RPA's and 2 LP's. The DPB receives commands from the spacecraft and controls the swept voltage set points. The APB interfaces directly with the sensors and sends the buffered/amplified analog current measurement signals to the DPB where it is buffered and processed and sent as telemetry to the spacecraft upon request. The LVPS block receives 28V bus power and provides the necessary input power to the DPB and APB.

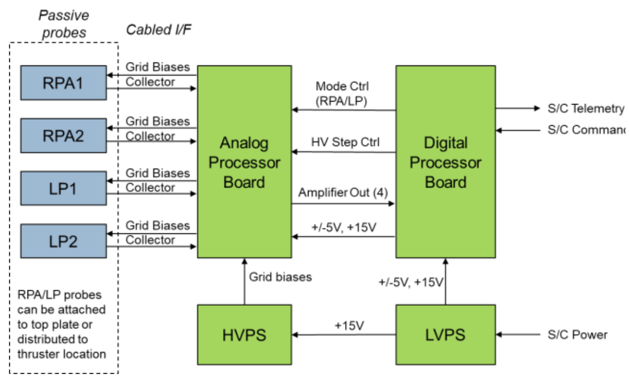

Figure 2. TIDBIT electronics system block diagram

B. Analog Processing Board & HVPS

A common analog front-end has been designed for interfacing with either Langmuir probes or RPA's, shown schematically in Fig. 3. The board provides a swept bias ranging from -50 to 950 V for the current-collecting electrode, with current measured by a low-side shunt resistor, labelled R_{sense}, and buffered/amplified by a high gain bandwidth (>100MHz) operational amplifier. The stray capacitance of the DC/DC converters used to control the collector bias must be kept low for applications desiring high temporal resolution for the current measurements in this low-side topology.

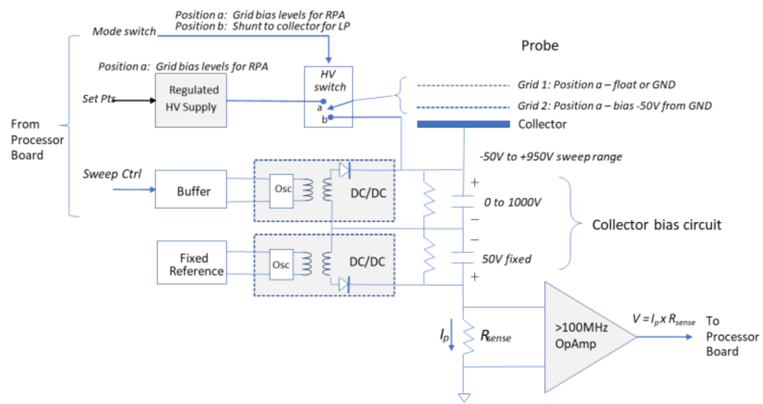

Figure 3. Analog electronics for a hybrid RPA/LP sensor

This circuit is all that is needed to make a standard LP measurement. Additional regulated power supplies are available to bias the grids of an RPA (e.g. Grid 2 in Fig. 3). The upstream grid or aperture for the RPA can be allowed to float or tied to spacecraft ground. A high voltage, double-pole/double-throw switch connects Grid 1 and Grid 2 to either their respective biasing circuits or to the collector. When both grids are connected to the collector the RPA can act as a planar Langmuir probe.

C. Digital Processing Board & LVPS

Control, data storage and bus interfacing are performed by the digital processing board. The amplifier output from the APB is first low-pass filtered then input to a 16-bit 100 Msps analog-to-digital converter (ADC) which is synchronized by a low-jitter 100 MHz clock. The ADC outputs are each buffered in RAM blocks of 10kS. The buffer can be expanded to 40kS if only one probe is used, allowing sufficient record length to capture a typical Hall thruster breathing cycle at 1Msps.

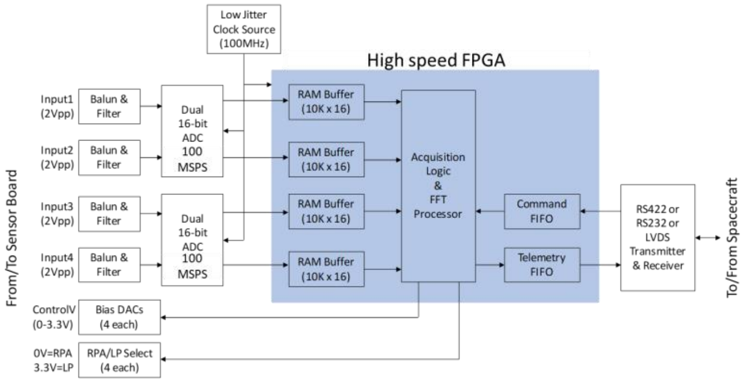

Figure 4. Example of digital electronics for RPA/LP sensor.

The FPGA can perform Fourier transform analysis of the high-speed signals and average the results over many cycles. This allows TIDBIT to transmit either temporal or spectral data depending on the command.

The DPB supports communication with the spacecraft over standard command and data interfaces such as UART, RS422 and LVDS.

D. Sensors

It is possible to incorporate a variety of diagnostics into the basic framework of the TIDBIT electronics package with little adjustment. Photodiodes, Hall probes, ExB probes and plasma wave detectors can be accommodated. The present work has focused on RPA's and LP's as they provide broadly useful information with minimal system complexity. A prototype sensor has been designed and tested which can be operated as a LP/RPA hybrid.

1. Prototype RPA Design

An initial design for an RPA was created which sought to incorporate the oft competing principles of simplicity and versatility. Standard RPA's constructed and utilized at The Aerospace Corporation implement a 3-grid design – here we have pared down to a single grid.

The present design eschews the normal entrance grid for a gridless entrance aperture plate which faces the plasma. The large area of the plate (35-mm diameter) compared to the aperture area (12.5-mm diameter) in the prototype allows for planar LP measurements to be made with this plate alone. The aperture is electrically isolated to allow biasing or floating – it can limit the impact of the probe on the local plasma potential and the aperture size may be adjusted based on desired collimation angle for ion collection. A grid may be attached to the aperture if needed – this is often done to reduce the space charge between the electron repelling and ion repelling grids, which is not necessary for a broad range of conditions if the gap between the two grids is small.

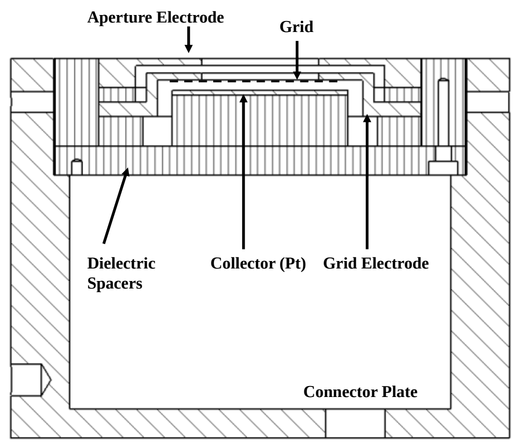

Figure 5. TIDBIT RPA/LP design

Downstream of the aperture plate is the electron repelling grid, spaced roughly 1-mm away. A 99.9% platinum weave mesh with 0.25-mm diameter apertures made from 0.06-mm diameter wires (65% open area) is attached to the aluminum grid electrode via spot welds spaced around the perimeter. The mesh is attached on the downstream side of the electrode, between the grid electrode and the collector. The mesh apertures are sized to handle plasma densities up to ~1×10^{17}-m^{-3}. The aperture and grid electrodes are shouldered to ensure that sputter products will not coat the dielectric spacers, which would otherwise result in high conductive currents.

The collector is a 0.5-mm thick, 19-mm diameter disc made from 99.95% pure platinum. The platinum electrode is attached via screws to an insulating spacer. The thickness of the spacer sets the gap width between the collector and electron repelling grid, which is 1-mm in the tested model. The gap width allows collection of up to ~1-mA/cm^2 for a 200-eV/q ion beam (the aperture area is 5 cm^2). The prototype has a wide geometric collection angle (~80° half angle) due to the small gaps between grids.

The choice of platinum for the grid and collector is motivated by the lack of a secondary-electron-suppression grid. Incident and reflected ions impinging on the collector and grid respectively induce electron emission from the metal surfaces which can lead to spurious currents. At the low ion kinetic energies studied here (<1keV) electron emission is predominantly due to Auger processes[9]. Auger neutralization requires the ionization energy of the impinging ion to be greater than twice the work function of the surface to result in electron ejection, i.e. $2\phi_w < E_i$ where ϕ_w is the work function and E_i is the ionization energy. Singly charged xenon ions have $E_i = 12.1$-eV, while platinum has a measured work function ranging from ~5.3-6.3 eV depending on conditions[10], making electron ejection by Auger neutralization unlikely. Hall thruster plumes contain an appreciable flux of higher charge state xenon ions which will have enough potential energy to result in electron ejection through Auger neutralization, so some electron emission is expected. Measurements of the electron yield are presented in the subsequent section.

III. Experiment

Measurements were performed comparing the TIDBIT RPA prototype to our standard 3-grid RPA design and a planar Langmuir probe in the far plume of a 1kW class Hall thruster operated at 300V. Experiments were performed in the EP2 vacuum chamber, with the probes inside the main, 2.4-m diameter chamber, and the thruster in an attached fiberglass chamber used for EMI measurements[8]. The thruster plume terminates at a pyramidal carbon beam dump 3.2-m downstream while the probes are translated laterally across the plume 2.2-m downstream of the thruster. The background pressure in the main chamber was 4×10^{-6} Torr corrected for xenon.

Measurements from the standard RPA, the TIDBIT RPA and the planar Langmuir probe were performed with the same Keithley 2410 source meters for consistency in comparison. The planar probe diameter is 13.5-mm which is close to the inlet aperture diameters of the two RPA's at 12.5-mm.

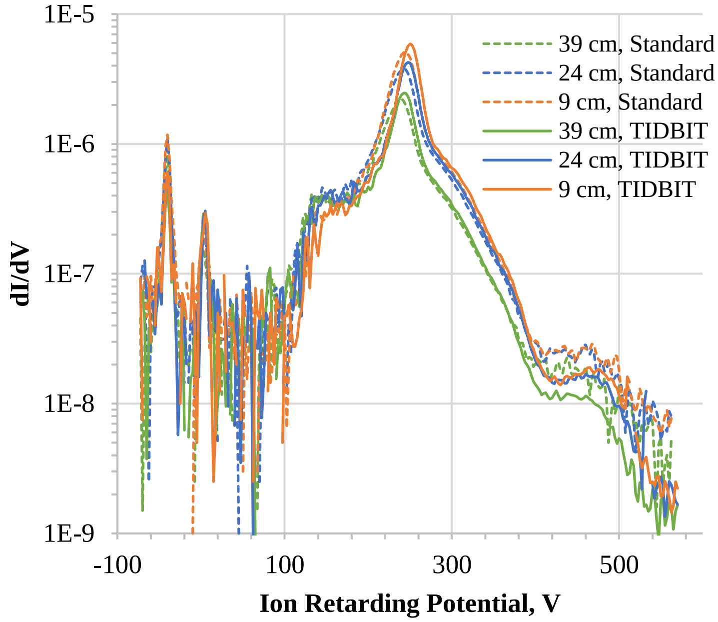

Figure 6. Ion energy-per-charge distributions measured 2.2-m downstream and at various lateral distances from thruster axis. Dashed line shows standard RPA (scaled) and solid line shows TIDBIT results

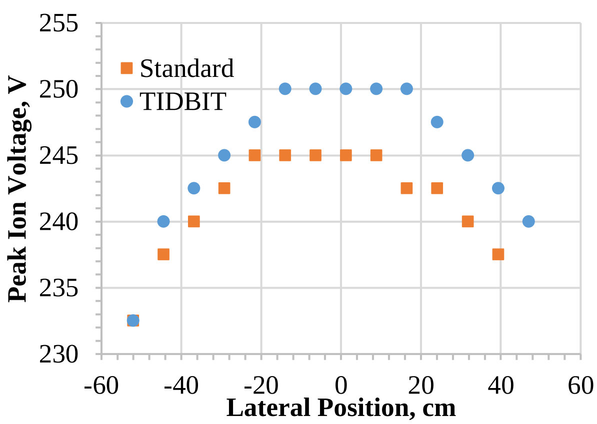

Figure 7. Most probable ion energy-per-charge measured 2.2-m downstream and at various lateral distances from the thruster axis

The TIDBIT RPA was biased to -40V on the grid and 0V on the aperture plate, while the collector bias was swept from -75 to 575V for the data shown here. The standard RPA was operated similarly, with the electron grid at -40V and the ion repelling grid and collector biased to the same potential. While the current to the ion grid and collector is measured separately, the two are added for the results shown here. All voltages are with respect to chamber ground, with the cathode floating to -20V during these tests.

A comparison of the ion energy per charge is shown in Fig.6 for the two RPA's. The standard RPA collects half as much current (when ion grid and collector are summed) as TIDBIT due to the decreased transparency of the multiple meshes. The standard RPA results are scaled in Fig. 6 by the least squares ratio of TIDBIT to standard RPA ion current at -10V ion repeller bias (this ratio is 1.99).

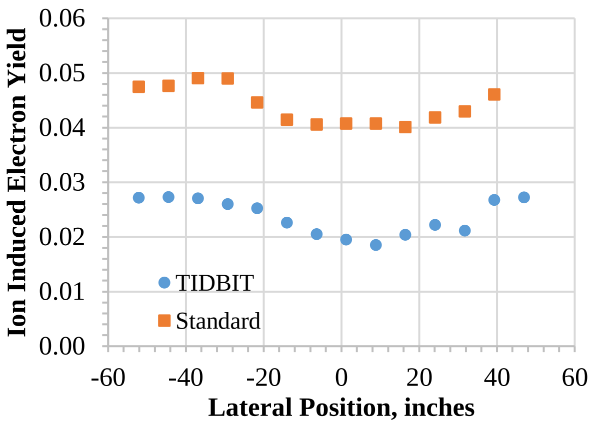

Figure 8. Effective ion induced electron yield for the RPA collector on the TIDBIT and standard probes

Both RPA's exhibit standard features of a Hall thruster plume[11]. There is a sharp peak at -40V which is due to the electrons emitted from the collector being re-collected at the emitting electrode once biased above the electron repeller. Another peak in the ion energy distribution occurs near +5V that is presumably from charge exchange ions, though at lower than expected energies. The planar LP measures local plasma potentials ranging from 6-7V which suggests the grid-to-collector gap is space charge limited at these low potentials for both the standard RPA and TIDBIT, though this is unexpected at the currents measured.

The most probable voltage for ions ranges from 230 to 250V for an anode voltage of 300V and cathode potential of -20V, as shown in Fig. 7. The most probable voltage measured by TIDBIT is always higher than that measured by the standard RPA, likely due to reduced space charge issues, which is supported by the convergence of the most probable voltage at -52-cm.

There is a shoulder in the ion energy distribution observed near 140V at all locations due to elastic scattering of ions off neutrals in the plume. This shoulder is well-captured by both probes with no apparent change in energy. There is an additional shoulder of slight prominence near double the most probable ion voltage (~470V) which is likely due to the portion of the doubly ionized xenon beam which gains an electron through charge exchange collisions while transiting the plume[11]. The slow drop in the ion voltage distribution function from 280 to 400 V may be a combination of triply charged beam ions which gain an electron in the plume and doubly charged ions undergoing both charge exchange and elastic scattering. Electron leakage may also play a role at these large biases.

We can directly estimate the ion induced electron emission yields from the change in collector current as the bias becomes greater than the electron repeller bias (-40V). A comparison of the effective yields for the standard and TIDBIT RPA's is given in Fig. 8 which suggests the electron yield is low in either case, but substantially lower for TIDBIT. A reduced yield is part of the TIDBIT design; however, the results of Fig. 8 do not represent a controlled comparison of yields due to the differing geometries of the two probes.

It is interesting to note that if the platinum collector truly eliminates singly charged xenon ion-induced electron emission then the yield measurement shown in Fig. 8 is a measure of the flux of multiply charged ions. We do not currently know the electron yield due to doubly charged xenon for our collector, but we can make a rough estimate from the semi-empirical scaling of Baragiola *et al*[12], $\gamma = 0.032(0.78E_i - 2\phi_w)$, which gives a yield of 0.48 for Xe^{2+} assuming a platinum work function of 5.3eV. This yield corresponds to a doubly charged xenon flux that is 5-7% of the singly charged ion flux based on the data in Fig. 8 and neglecting the flux of triply charged xenon. Triply charged xenon may safely be neglected if its flux is <15% the flux of doubles.

A comparison of the planar LP with TIDBIT in LP mode is shown in Fig. 9. The largest discrepancy appears in electron density which is determined by integrating the measured EEDF over velocity (assuming the 1D EEDF is symmetric). The 1-D EEDF is determined from the first derivative of the probe current with respect to voltage and is also used to determine the average axial kinetic energy[13]. The reason for the noticeable discrepancies in potential and density is unclear but may be related to differences in probe perturbations to the local plasma. The TIDBIT prototype is 5.1-cm in outer diameter compared to 1.9-cm outer diameter for the LP.

It would be of interest to test a smaller TIDBIT, both to determine the extent to which plasma perturbations alter the LP-mode results and to allow for closer placement of the TIDBIT sensor to the thruster. The prototype sensor was not built for compactness and it should be straightforward to reduce its outer dimensions while retaining high signals.

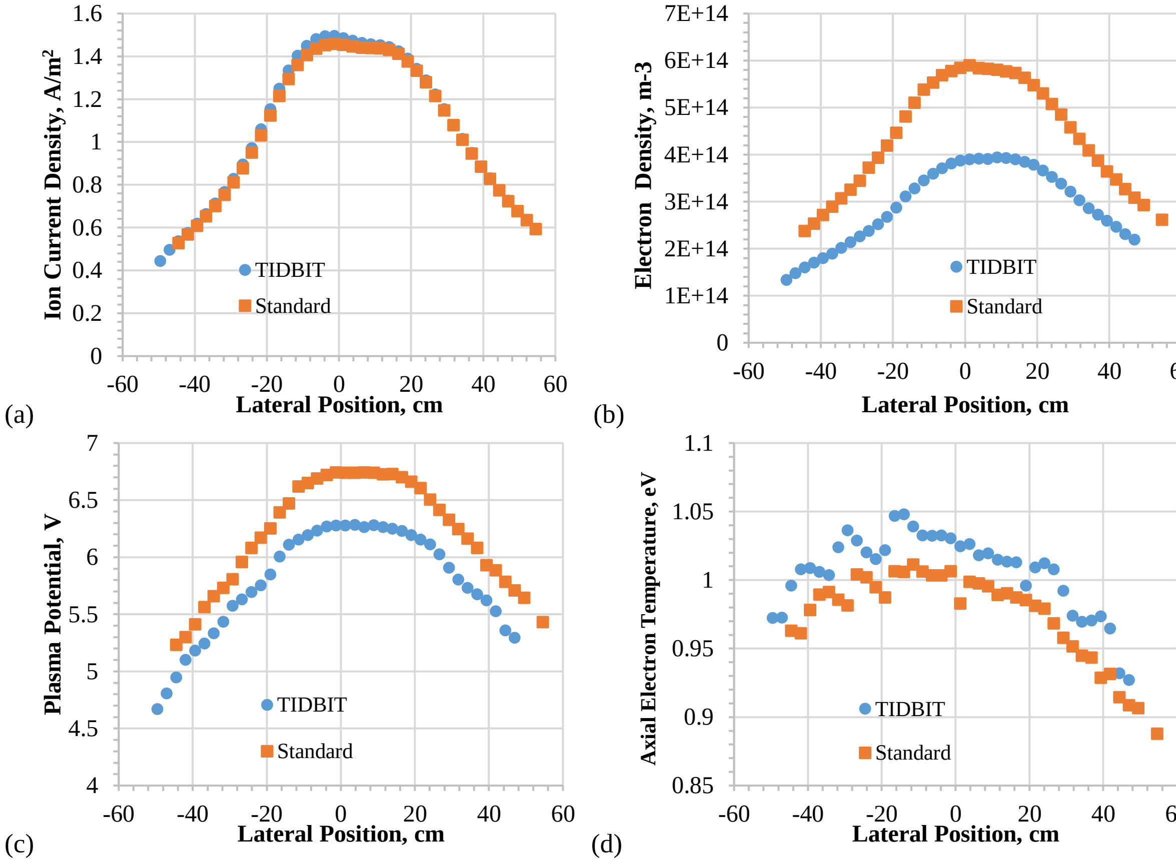

Figure 9. Comparison of plasma parameters measured by standard planar LP and TIDBIT aperture plate. (a) Ion current density (b) plasma density (c) plasma potential and (d) average axial electron energy

IV.Conclusion

Facility Effects remain a critical issue for the qualification of new EP systems, particularly as power levels expand and a variety of unique options emerge. A major impediment to progress in the field of study of Facility Effects is the noted dearth in on-orbit plasma characterization. This dearth is to be expected. There is scant motivation for any flight (other than perhaps technology demonstrations) to spend considerable resources (mass, space, time, and price) on the collection of engineering data for the broader EP community with little perceived impact on mission. It may become worth the investment if the costs (in mass, space, time and price) decrease and the mission impact – through the collection of useful advanced thruster health telemetry – increases.

A program was initiated at TAC to design a flight diagnostic that would be cheap, small and simple to implement so that advanced indicators of thruster health can be commonly monitored, and the much-needed ground-test-comparison data may be collected. A conceptual design was presented which included a high speed analog front-end built around a 4 sensor, RPA/LP, architecture. The analog board is coupled to an FPGA-based digital processing board which interfaces with the spacecraft bus and upholds a do-no-harm priority.

We also presented a prototype RPA/LP sensor with a unique design, intended to maximize probe signals while maintaining sensitivity. In certain circumstances this probe can yield information about the charge state ratios as well. The TIDBIT prototype sensor performed superior to the standard laboratory RPA utilized at TAC in comparison testing on a Hall thruster operated at 300V – yielding double the signal (for the same inlet aperture) while simultaneously reducing sensitivity to space charge. Next steps include prototype builds of the APB and DPB which will undergo end-to-end testing with a miniaturized version of the present sensor proximal to a Hall thruster.

Acknowledgments

The authors would like to thank Philip Mak and Michael Nakles for performing much of the mechanical design work and assembly of the probe and for setting up the experiment. The probe was fabricated by Mike Worshum. This work was partially supported under The Aerospace Corporation's Independent Research and Development program.

References

[1]Byers, D., and Dankanich, J.W., "A Review of Facility Effects on Hall Effect Thrusters," *IEPC 2009-076*.

[2]Diamant, K., Spektor, R., Beiting, E.J., Young, J.A., and Curtiss, T.J., "The Effects of Background Pressure on Hall Thruster Operation", *AIAA Meeting Paper AIAA-2012-3735*, Atlanta, GA, 2012.

[3]Diamant, K., Lee, T., Liang, R., Noland, J., Vial, V., Cornu, N. "Performance and Plume Characterization of the PPS®1350-G Hall Thruster", *AIAA Meeting Paper AIAA-2016-4543*, Salt Lake City, UT, 2016.

[4]Diamant, K., Liang, R., and Corey, R.L., "The Effect of Background Pressure on SPT-100 Hall Thruster Performance," *AIAA Meeting Paper AIAA-2014-3710*, Cleveland, OH, 2014.

[4]Hofer, R.R., and Anderson, J.R., Finite Pressure Effects in Magnetically Shielded Hall Thrusters," *AIAA Meeting Paper AIAA-2014-3709*, Cleveland, OH, 2014.

[5]Nakles, M.R., and Hargus, W.A., Jr., "Background Pressure Effects on Ion Velocity Distribution Within a Medium-Power Hall Thruster," *Journal of Propulsion & Power*, Vol. 27, No. 4, Jul-Aug 2011, pp. 737,743.

[6]Spektor, R., Tighe, W.G., and Kamhawi, H., "Laser Induced Fluorescence Measurements in a Hall Thruster Plume as a Function of Background Pressure", *AIAA Meeting Paper AIAA-2016-4624*, Salt Lake City, UT, 2016.

[7]Randolph, T., Kim, V., Kaufman, H., Kozubsky, K., Zhurin, V., and Day, M., "Facility Effects on Stationary Plasma Thruster Testing", *IEPC 1993-93*.

[8]Beiting, E.J., and Garrett, M.L., "Facility for High-fidelity Electromagnetic Compatibility Studies of Electric Thrusters," *AIAA Meeting Paper AIAA-2007-5329*, Cincinnati, OH, 2007.

[9]Hagstrum, H.D., "Theory of Auger Ejection of Electrons from Metals by Ions," *Physical Review*, Vol. 96, No. 2, 1954.

[10]Kawano, H., "Effective work functions for ionic and electronic emissions from mono- and polycrystalline surfaces," *Progress in Surface Science*, Vol. 83, 2008, pp.1-165.

[11]Pollard, J.E., Diamant, K.D., Khayms V., Werthman, L. King, D.Q., de Grys, K.H., "Ion flux, energy, and charge-state measurements for the BPT-4000 Hall thruster", *AIAA Meeting Paper 2001-3351*, Salt Lake City, UT, 2001.

[12]Baragiola, R.A., Alonso, E.V., Ferron J., Oliva-Florio, A., "Ion-induced electron emission from clean metals", *Surface Science*, Vol. 90, 1970, pp. 240-255.

[13]Woods, R.C., and Sudit, I.D., "Theory of Electron Retardation by Langmuir Probes in Anisotropic Plasmas," *Physical Review E*, Vol. 50, No. 3, Sep 1994, pp. 2222,2238.

[14]Wang, J., Brinza, D.E., Young, D.T., Nordholt, J.E., Polk, J.E., Henry, M.D., Goldstein, R., Hanley, J.J., Lawrence, D.J., Shappirio, M., "Deep Space One investigations of ion propulsion plasma environment," *Journal of Spacecraft and Rockets,* Vol. 37, No. 5, 2000, pp.545-555.

[15]Manzella, D., Jankovsky, R., Elliott, F., Mikellides, I., Jongeward, G., Allen, D., "Hall thruster plume measurements on-board the Russian Express satellites," *NASA/TM-2001-211217,* 2001.

[16]Tajmar, M., Meissl, W., Gonzalez del Amo, J., Foing, B., Laakso, H., Noci, G., Capacci, M., Malkki, A., Schmidt, W., Darnon, F., "Charge-exchange plasma contamination on SMART-1: first measurements and model verification," *AIAA Meeting Paper AIAA-2004-3437*, Fort Lauderdael, FL, 2004.

[17]Johnson, L., De Soria-Santacruz Pich, M., Huang, W., Choi, M., Sekerak, M.J., "Flight plasma diagnostics for high-power, solar-electric deep-space spacecraft," *IEEE Aerospace Conference*, Big Sky, MT, 2018.

[18]Bromaghim, D., Reed, G., Singleton, J., Connolly, D., Johnson, L., Conroy, D., Gorecki, R., an, F.D., Choy, H., Pote, B., Byrne, L.T., Connolly, W.J., Hruby, V.H., Barbarits, K., Syndey, P.F., Hamada, K.M., Dressler, R.A., Chiu, Y.H. , "Summary of on-orbit performance of the 200-W Hall thruster system on TacSat-2," *JANNAF J. Propuls. Energ.,* Vol. 4, No. 1, 2011, pp.87-102.